HAO1-Mediated Oxalate Metabolism Promotes Lung Pre-Metastatic Niche Formation by Inducing Neutrophil Extracellular Traps

Zhicheng Zeng
Shunde Hospital of Southern Medical University

Shaowan Xu
Southern Medical University

Feifei Wang
Southern Medical University

Xin Peng
Southern Medical University

Wanning Zhang
Southern Medical University

Yizhi Zhan
Southern Medical University

Yanqing Ding
Southern Medical University

Ziguang Liu
Shunde Hospital of Southern Medical University

Li Liang (✉ lli@smu.edu.cn)
Southern Medical University Nanfang Hospital   https://orcid.org/0000-0003-2424-4926

Research

Abstract

Background

Metabolic reprogramming has been shown to be involved in cancer-induced PMN formation, but the underlying mechanisms have been insufficiently explored.

Methods

HAO1 expression in lung tissues and alveolar epithelial cells were deteted by qPCR and Western blotting. The effect of HAO1 on the lung metastasis of cancer was investigated by orthotropic metastasis assay. Lungs and cells oxalate levels were determined using an oxalate assay kit. The effect of oxalate on neutrophil extracellular trap formation was investigated by immunofluorescence. The effect of oxalate on proliferation of breast cancer cells was revealed by immunofluorescence by colony formation assay.

Results

HAO1 was up-regulated in the alveolar epithelial cells of mice bearing metastatic breast cancer cells at the pre-metastatic stage. Upregulation of HAO1 led to oxalate accumulation in lung tissues and alveolar epithelial cells. Pharmacologic inhibition of HAO1 could effectively suppress the lung oxalate accumulation induced by primary cancer. Lung oxalate accumulation induced NET formation by activating NADPH oxidase. Lung oxalate accumulation promoted the proliferation of metastatic cancer cells by activating the MAPK signaling pathway. Breast cancer cells induced HAO1 expression and oxalate accumulation in alveolar epithelial cells by activating TLR3-IRF3 signaling.

Conclusion

These findings underscore the role of HAO1-mediated oxalate metabolism in cancer-induced lung PMN formation and metastasis. HAO1 could be an appealing therapeutic target for preventing lung metastasis of cancer.

Background

Alteration of microenvironmental signals occurring before the arrival of disseminating cancer cells contributes to distant metastasis of cancer, which is termed the PMN. Metabolic reprogramming is an important characteristic of the PMN that empowers the niche to favor cancer cell colonization and promote metastasis[1]. Primary tumors may modify the metabolic reprogramming of non-tumor cells within the PMN. For example, breast cancer secreted miR-122 reprograms glucose metabolism in the

PMN to promote metastasis[2]. However, little is known about how metabolic reprogramming modulates PMN formation.

Oxalate is an inert metabolic end product that is synthesized by a variety of cells, such as liver cells, epithelial cells and apocrine cells[3]. Oxalate accumulation leads to ROS-induced oxidative stress and tissue injury by activating NADPH oxidase[4, 5]. In addition, a previous study has suggested that oxalate promotes the proliferation of breast cancer[6]. HAO1 is a rate-limiting enzyme of oxalate synthesis that catalyzes the oxidation of glycolate to glyoxylate and glyoxylate to oxalate[7, 8]. Pharmacologic inhibition or knockdown of HAO1 is an efficient approach to reduce oxalate production[9–12]. However, the functional role of HAO1-mediated oxalate metabolism in cancer development remains unclear.

Neutrophil extracellular traps (NETs), scaffolds of decondensed chromatin coated with cytotoxic enzymes and proteases, are produced in neutrophils and can be released into the extracellular matrix to trap microorganisms[13]. Pathogen-induced NET formation is primed by activation of the NADPH oxidase enzyme complex[13]. Interestingly, a growing body of evidence suggests that tumor cells are able to stimulate NET formation in the absence of infection, which contributes to cancer development and metastasis[14]. Primary tumors induces NET formation at foreign sites before metastasis, leading to PMN formation[15]. In addition, NETs can trap disseminating tumor cells, which contributes to early adhesion of tumor cells to foreign sites[16]. NETs shield tumor cells against cytotoxic T lymphocytes and NK cells, thus hampering tumor clearance[17]. NET-DNA can act as a chemotactic factor to attract cancer cells dispersed from their primary site, which is essential for metastasis formation[18]. These studies highlight the important role of NETs in cancer progression, but the mechanisms through which cancer cells modulate NET formation in the PMN have been insufficiently explored.

TLR3, a toll-like receptor, is located inside the cell in endocytic compartments and the endoplasmic reticulum, and recognizes dsRNA[19] and exosome transfer RNA[20]. Recent studies have underscored the pivital role of TLR3 in cancer metastasis. Tumor exosomal RNA contribute to host lung epithelial cell TLR3 activation, which is predominantly expressed by alveolar epitherlial cells in pre-metastatic lung, inducing neutrophil recruitment and lung metastatic niche formation[21]. Tumor-derived dsRNA induces endothelial slit2 expression,which promotes the migration of cancer cells toward endothelial cells and drives metastatic progression[22].

In this study, we show that metastatic breast cancer cells induce HAO1 expression in alveolar epithelial cells by activating TLR3-IRF3 signaling, rendering an over-production of oxalate. Oxalate accumulation in the lung initiates PMN formation by inducing NETs. In addition, oxalate promotes the proliferation of metastatic cancer cells by activating MAPK signaling. Most importantly, pharmacologic inhibition or knockdown of HAO1 alleviates the pro-metastatic effect of oxalate accumulation.

Methods

Cell culture and treatment

MCF7, MDA-MB-231, 67NR and 4T1 cells were obtained from ATCC. All cells were cultured in Dulbecco's modified Eagle's medium (DMEM, Gibco) with 10% fetal bovine serum Gibco), 1% penicillin and streptomycin, and they were maintained at 37 °C and 5% CO_2. MCherry-expressing 4T1 cells were established by transfection with lentivirus expressing mCherry. Potassium oxalate (20 μM, Aladdin), DNAse I (100 U/ml, Aladdin), CCPST (200 μM, Key organics), PMA (10 nM, MedChemExpress), apocynin (10 μM, MedChemExpress), SB 203580 (500 nM, MedChemExpress) and CU CPT 4a (27 μM, Tocris) were used for cell treatment.

Isolation of neutrophils and alveolar epithelial cells

For isolation of neutrophils, bone marrow cells derived from 6 to 8-week-old BALB/c mice were harvested in Hank's buffered salt solution (HBSS, Gibco), subsequently filtered through 40-μm nylon mesh and added to the top of a 2-layer Percoll (GE Healthcare) gradient (72% and 65% in PBS), followed by centrifugation at 800 g for 20 min at 4 °C. Neutrophils enriched in the interface of 65%-72% fractions were confirmed to be of >95% purity by immunofluorescence (Supplementary figure S1H). For isolation of alveolar epithelial cells, BALB/c mice were perfused with 5 ml of HBSS through the pulmonary artery via the right ventricle and instilled with 4.5 U/ml of elastase (Roche Diagnostics) via tracheal cannula. The lung lobes were then minced in 100 U/ml DNase I (Aladdin). Cells in suspension were subsequently filtered through 40 μm nylon mesh and then enriched by IgG panning. The purified alveolar epithelial cells were confirmed to be of >90% purity by immunofluorescence (Supplementary figure 3F).

Mice and Tumor Models

6 to 8-week-old female BALB/c, C57BL/6 and athymic mice were used in all animal experiments. All protocols for the animal studies were approved by the Institutional Animal Care and Use Committee of Southern Medical University. For the orthotropic metastasis assay of breast cancer, MCF7, MDA-MB-231 (1×10^6 cells) were injected into the fourth mammary fat pad of athymic mice, and 67NR (1×10^6 cells) and 4T1 cells (1×10^5 cells) were injected into the fourth mammary fat pad of BALB/c mice. For the orthotropic metastasis assay of CRC, CMT93 cells (1×10^6 cells) were injected into the mesentery at the tail end of the cecum of C57BL/6 mice. For the orthotropic metastasis assay of HCC, HCCLM3 cells (1×10^6 cells) were injected into the liver of athymic mice. For the tail vein metastasis assay, 5×10^5 4T1 cells were injected into the tail vein of mice. For oxalate or poly(I:C) administration, mice inhaled potassium oxalate (20 mg/ml) three-times daily for 20 min or once daily with exposure to poly(I:C) (2 mg/ml dissolved in PBS) for 20 min. For CCPST administration, mice received an intraperitoneal injection of CCPST (10 mg/kg) once daily. For AAV administration, mice were injected with 10^{11} vg AAV6-control sgRNA or AAV6-Hao1 sgRNA (with HA-tag, GeneCopoeia, the sequences are shown in Supplementary Table 1) diluted in 100 μl PBS, respectively, via the tail vein.

Western blot

Tissue and cells were lysed with RIPA buffer (Fdbio science) and quantified using the Bradford Protein Assay (KeyGEN BioTECH). Equal amounts of extracts were subjected to SDS–PAGE, and transferred onto nitrocellulose membranes (Millipore). Then, the membranes were incubated with primary antibodies overnight at 4°C. The following primary antibodies were used: HAO1 (Immunoway, YM3378, 1:1000 dilution), GAPDH (Proteintech, 60004-1-Ig, 1:5000 dilution), mCherry (Abcam, ab213511, 1:2000 dilution), TSG101 (Proteintech, 14497-1-AP, 1:1000 dilution), IRF3 (Proteintech, 11312-1-AP, 1:1000 dilution), p-IRF3 (Affinity, AF3438, 1:1000 dilution), p38 (Cell signaling technology, #8690, 1:1000 dilution) and p-p38 (Cell signaling technology, #4511, 1:1000 dilution). Following incubation with the HRP-conjugated antibody (Fdbio science, FDM007 or FDR007, 1:10000 dilution). Bands were detected using FDbio-Femto ECL Western blotting detection reagents (Fdbio science)

QPCR and RNA Sequencing

Total RNA was extracted from tissue and cells using TRIzol reagent (Clontech Laboratories) according to the manufacturer's instructions. Reverse transcription was performed using PrimeScript™ RT Master Mix (Clontech Laboratories). Quantitative real-time PCR analysis was performed using SYBR Green PCR Master Mix (TaKaRa). The sequences of all indicated primers are listed in Supplementary Table 2. For RNA sequencing, the enriched mRNA from 4T1 cells treated with or without potassium oxalate (20 μM) was reverse transcribed into cDNA. The cDNA libraries were sequenced on the Illumina sequencing platform by Genedenovo Biotechnology Co., Ltd (Guangzhou, China). The data are deposited at the Gene Expression Omnibus (accession number: GSE166167).

Immunofluorescence

Paraffin-embedded tissue blocks were cut into 2.5-μm sections and transferred to glass slides. Sections were immersed in 3% hydrogen peroxide and incubated with primary antibodies overnight at 4°C. Subsequently, sections were stained with goat anti-mouse and anti-rabbit IgG/Alexa Fluor (Bioss Antibodies). The following primary antibodies were used: HAO1 (Immunoway, YM3378, 1:200 dilution), SP-C (Proteintech, 10774-1-AP, 1:200 dilution), mCherry (Abcam, ab213511, 1:500 dilution), citrullinated histone H3 (Abcam, ab5103, 1:200 dilution), MPO (R&D Systems, AF3667, 1:200 dilution), neutrophil elastase (Abcam, ab131260, 1:200 dilution).

Fluorescence-activated cell sorting

BALB/c mice were perfused with 5 ml of HBSS through the pulmonary artery via the right ventricle and instilled with 4.5 U/ml of elastase (Roche Diagnostics) via tracheal cannula. The lung lobes were then minced in 100 U/ml DNase I (Aladdin). Cells in suspension were subsequently filtered through a 40 μm nylon mesh and then sorted by FACS. Anti-CD45 (BioLegend, 157607, 1:200 dilution) and anti-CD3 (BioLegend, 100209, 1:200 dilution) antibodies were used for the isolation of T cells. Anti-CD45 and anti-CD19 (BioLegend, 152407, 1:200 dilution) antibodi were used for isolation of B cells. Anti-CD45 and anti-NK-1.1 (BioLegend, 108703, 1:200 dilution) antibody were used for isolation of NK cells. Anti-CD45 and anti-F4/80 (BioLegend, 123105, 1:200 dilution) antibodies were used for the isolation of macrophages.

Anti-CD45 and anti-Ly6G (BioLegend, 127627, 1:200 dilution) antibodies were used for the isolation of neutrophils. Anti-EpCAM (BioLegend, 324215, 1:200 dilution) and anti-SP-C (abclonal, A1835, 1:500 dilution) antibodies were used for the isolation of alveolar epithelial cells. Anti-CD31 (BioLegend, 102409, 1:200 dilution) antibody was used for the isolation of endothelial cells. Anti-S100A4 (abcam, ab197896, 1:500 dilution) antibody was used for the isolation of fibroblasts.

Determination of th oxalate concentration in lungs and cells

Lung and cell oxalate levels were determined using an oxalate assay kit (Biovision, K663). A total of 5 mg lung tissue or 5×10^5 cells was ground and resuspended in 100 µl Oxalate Assay Buffer, following by a centrifution at 12,000 rpm for 10 min. The supernatant was collected for oxalate detection. The reaction mix was added and incubated at 37°C for 30 min. The OD (at 450 nm) was measured.

Colony formation assay

A total of 500 cells were plated in each well of 6-well plates and were cultured in DMEM with 2% fetal bovine serum. The medium was renewed every 3 days. After 10 days, the cells were fixed using 4% paraformaldehyde for 30 min, stained with hematoxylin for 30 min and then photographed.

Purification of NETs and transwell migration assay

Neutrophils were treated with 20 nM PMA or 20 nM PMA plus 20 µm potassium oxalate for 4 h. NETs adhering to the bottom of the well were then washed with DMEM containing 2% fetal bovine serum and were centrifuged at 1000 ×g at 4 °C for 10 min. The supernatant containing NETs was collected. Subsequently, 5×10^4 cells were suspended in serum-free DMEM and seeded into the transwell chambers with 8-µm-pore-size inserts (BD Biosciences). The medium containing NETs with or without DNAse I (100 U/ml) was placed into the bottom chamber. After 6 h, the cells that had migrated through the membrane and stuck to the lower surface of the membrane and were counted as cells per field of view under light microscopy.

Adherence assay

A total of 5×10^5 neutrophils were plated in 24-well plates and treated with 20 nM PMA, 20 nM PMA plus 20 µm potassium oxalate or 20 nM PMA plus 20 µm potassium oxalate and 100 U/ml DNAse I for 4 h. MCherry-expressing 4T1 cells (1×10^5) were added to each well and were allowed to adhere to the plate bottom for 15 min. Subsequently, the wells were fixed using 4% PFA. Adherent cells were stained with anti-mCherry, and the number of mCherry-expressing 4T1 cells was counted as cells per field of view under confocal microscopy.

NET formation assay

Neutrophils were treated with 20 nM PMA or 20 nM PMA plus 20 µm potassium oxalate for 4 h. Then, the neutrophils were fixed with 4% PFA and than stained with anti-MPO and anti-citrullinated histone H3. NET

formation was determined as the percentage of the field of view positive for a citrullinated histone H3.

ROS analysis

Neutrophils were treated with 20 nM PMA, 20 nM PMA plus 20 μm potassium oxalate or 20 nM PMA plus 20 μm potassium oxalate and 10 μM apocynin for 2 h. Subsequently, the cells were incubated with 10 mM CM-H2DCFDA (Yeasen), for 15 min and then washed with pre-chilled PBS, and the fluorescence of each well was monitored at 480 nm excitation and 540 nm emission.

Isolation, identification and treatment of exosomes

Exosomes were derived from breast cancer cell conditioned media by ultracentrifugation. Breast cancer cells were cultured in DMEM medium with 10% fetal bovine serum, which was depleted of exosomes by ultracentrifugation at 120,000 x g for 8 h at 4°C prior to use. Conditioned media were centrifuged at 500 x g for 10 min at 4°C, followed by 16,800 x g for 30 min at 4°C. The supernatants were passed through a 0.22-μm filter (Millipore) and ultracentrifuged at 120,000 x g for 70 min at 4°C. The exosomes were washed with PBS and then resuspended in PBS. The amount of exosomes was determined by the Bradford Protein Assay (KeyGEN BioTECH). Transmission electron microscopy was performed as as previously described[23]. For cell treatment, a total of 5 μg exosomes were incubated with $5×10^5$ recipient cells for 48 h.

Results

HAO1 is up-regulated in alveolar epithelial cells within the lung PMN

To gain insight into metabolic changes induced by primary cancers in the pre-metastatic lung, we analyzed public gene expression profiles of lungs from mice without any tumors and mice bearing non-metastatic (67NR) or metastatic (4T1) breast cancer cells in the pre-metastatic phase (GSE62817)[24]. Among the differentially expressed genes, four metabolic-associated genes (HAO1, MGAM, BCHE, and TYMS) were selected for further study (Supplementary figure 1A).

Orthotopic implantation of mCherry-labeled 4T1 and MDA-MB-231 cells into mice resulted in the development of lung metastases 5 and 7 weeks later, respectively (Supplementary figure 1B-E). Thus, we detected the four candidate genes in lung PMNs in the second week after orthotopic implantation of non-metastatic breast cancer cell lines (67NR and MCF7) and metastatic cell lines (4T1 and MDA-MB-231). RT-PCR analyses showed that HAO1 was the most significantly up-regulated gene in lung PMN (Figure 1A and B). Western blot analysis confirmed that HAO1 gradually increased from the first week to the fifth week in mice bearing 4T1 cells (Figure 1C). Interestingly, we found that orthotopic implantation of metastatic breast cancer cell lines up-regulated HAO1 expression only in lung PMNs, but not in brain, bone or liver PMNs (Supplementary figure 1F). We then explored whether primary colorectal cancer (CRC) and hepatocellular carcinoma (HCC) could regulate HAO1 expression in the lung PMN. Orthotopic implantation of the CRC cell line CMT93 and HCC cell line HCCLM3 led to the development of lung

metastases 6 and 4 weeks later, respectively (Supplementary figure 1G and H). Markedly elevated HAO1 expression was observed in the lung PMN at the second week after orthotopic implantation of CMT93 and HCCLM3 cells (Supplementary figure 1I and J). Subsequently, we performed fluorescence-activated cell sorting (FACS) to isolate alveolar epithelial cells, B cells, endothelial cells, macrophages, fibroblasts, neutrophils, NK cells and T cells from lungs of 4T1-bearing mice. QPCR analysis showed that HAO1 was dramatically up-regulated in alveolar epithelial cells from mice inoculated with 4T1 cells (Figure 1D). Immunofluorescence analysis in lungs from 4T1-bearing mice further corroborated the colocalization of HAO1 and SP-C, a specific marker of alveolar epithelial cells (Figure 1E). Congruently, alveolar epithelial cells in 4T1-bearing mice showed a higher expression of HAO1 compared with those in mice without tumor (Figure 1E). Furthermore, we performed immunofluorescence to detect HAO1 expression in lung tissue derived from three breast cancer patients with lung metastases and three patients with pulmonary bulla. Higher expression of HAO1 was observed in alveolar epithelial cells from breast cancer patients with lung metastases than in those from patients with pulmonary bulla (Figure 1F, Supplementary figure 2A). We also cocultured alveolar epithelial cells with breast cancer cells in vitro (Supplementary figure 2B). Strikingly, alveolar epithelial cells cocultured with metastatic 4T1 and MDA-MB-231cells showed higher expression of HAO1 than the control or those co-cultured with non-metastatic 67NR and MCF7 cells (Figure 1G and H, Supplementary figure 2C and D). These results indicated that HAO1 was up-regulated in alveolar epithelial cells at pre-metastatic stage.

Pharmacologic inhibition or knockdown of HAO1 dampens lung PMN formation and metastasis

To evaluate the role of HAO1 in the formation of lung PMNs and lung metastasis, an AAV6 vector was applied to deliver Hao1 sgRNA to the lungs of the mice before inoculation of 4T1 cells into fat pad. A significant reduction of HAO1 in lung tissue was observed in AAV6-Hao1 sgRNA-infected mice at pre-metastatic stage (Supplementary figure 3A and B). The numbers of lung metastases were then detected 40 days after inoculation of 4T1 cells, with fewer pulmonary metastatic foci in AAV6-Hao1 sgRNA-infected mice (Figure 2A). CCPST is a specific inhibitor of HAO1 and has been used for substrate reduction therapy in a mouse model of primary hyperoxaluria Type 1[10]. We thus applied CCPST to block the function of HAO1 in tumor-bearing mice. CCPST was intraperitoneally injected into mice once a day after inoculation of 4T1 cells into the fat pad. Markedly reduction in lung metastases was observed in mice treated with CCPST (Figure 2B). However, there was no difference in primary tumor growth between the CCPST and control groups (Supplementary figure 3C). To further determine whether CCPST hampers cancer-induced PMN formation in the lung, mCherry-expressing 4T1 cells were injected into the tail vein of mice 2 weeks after the inoculation of unlabeled 4T1 cells into the fat pad and once daily administration of CCPST. The results showed that administration of CCPST resulted in a dramatic reduction of mCherry-expressing lung metastatic colonization (Figure 2C). In addition, we assessed the effect of CCPST on lung metastases of CRC and HCC in vivo, and the results showed that CCPST treatment also attenuated lung metastases in mice orthotopically implanted with CMT93 and HCCLM3 cells (Supplementary figure 3D and 3E). Collectively, these results illustrated that blockade of HAO1 prevented lung PMN formation and metastasis.

HAO1 promotes oxalate production in the lung PMN

HAO1 is a rate-limiting enzyme of oxalate synthesis. Thus we asked whether primary cancer could regulate oxalate production in the lung PMN. Two weeks after orthotopic implantation of breast cancer cell lines in fat pads, we detected the oxalate concentration in the lungs. The results showed that mice implanted with 4T1 and MDA-MB-231 cells generated higher pulmonary oxalate concentration than those without tumors and those bearing MCF7 and 67NR cells (Figure 3A and B). In vitro, increased production of oxalate was observed in alveolar epithelial cells cocultured with 4T1 and MDA-MB-231 cells. To confirm that oxalate accumulation induced by primary cancer was HAO1 dependent, we performed a once daily injection of CCPST after orthotopic implantation of 4T1 cells in the fat pad, or injection of sgHao1 AAV via the tail vein the day before orthotopic implantation of 4T1 cells in the fat pad, and then detected the pulmonary oxalate concentration after two weeks. The results showed that both CCPST and HAO1 knockdown suppressed oxalate production in lung PMN induced by primary cancer (Figure 3D and E).

To ascertain whether oxalate accumulation in lung tissue affected PMN formation and lung colonization of breast cancer cells in vivo, we performed a three-times daily inhalation of oxalate in mice, which led to an elevated oxalate concentration in mouse lungs (Supplementary figure 4). One week later, mCherry-labeled 4T1 cells were injected via the tail vein into the mice. The results showed that oxalate accumulation promoted lung metastatic colonization compared with the control (Figure 3F). Oxalate accumulation is capable of inducing inflammation[25]. Thus, we dectected the expression of proinflammatory factors COX2, IL1B, IL6 and TNFa, pro-metastatic factors Bv8, MMP9, S100a8 and S100a9[21] in the lung from mice inhalated with oxalate. As shown in Figure 3G, oxalate inhalation resulted in marked upregulation of proinflammatory factors and prometastatic factors in mouse lungs. The above data suggested that HAO1-induced oxalate accumulation was involved in lung PMN formation.

HAO1-induced oxalate accumulation elicits the formation of NETs

We next examined the changes in inflammatory cellular composition within lung PMNs induced by oxalate accumulation. We analyzed the number of many kinds of inflammatory cells including macrophages, neutrophils, B lymphocytes and T lymphocytes, in lung tissue from mice that inhaled oxalate. Immunofluorescence analyses confirmed that aerosol inhalation of oxalate in mice led to significant neutrophil recruitment (Figure 4A, supplementary figure 5A-D). In contrast, CCPST treatment dramatically reduced the number of pulmonary neutrophils in 4T1-bearing mice (Supplementary figure 5E). Previous studies have suggested that oxalate induces overproduction of ROS by activating NAPDH oxidase[4]. ROS production in neutrophils induced by the activation of the NADPH oxidase is considered an initial step in NET formation[13], which plays an important role in cancer metastasis. Thus, we postulated that NETs might contribute to oxalate-induced PMN formation in the lung. To confirm this hypothesis, neutrophils were isolated from the bone marrow of mice (Supplementary figure 5F) and treated with oxalate in vitro. Immunofluorescence staining showed that oxalate treatment led to NET formation

(Figure 4B). Increased ROS production in neutrophils was also observed under the oxalate treatment. However, apocynin, an inhibitor of NAPDH oxidase, effectively reduced ROS production in neutrophils stimulated by oxalate (Figure 4C). We also explored the effect of HAO1-induced oxalate accumulation on the formation of NETs in vivo. The results showed that the accumulation of oxalate in lung tissue induced NET formation (Figure 4D). Conversely, CCPST treatment suppressed pulmonary NET formation in 4T1-bearing mice (Figure 4E). These results demonstrated that HAO1-induced oxalate accumulation contributes to NET formation in the lung PMN.

NET-mediated cell trapping facilitates early adhesion of cancer cells to foreign sites[16]. Thus, we examined whether oxalate-induced NET formation could promotes the adhesion of cancer cells. As shown in Figure 4F, exposure of neutrophils to oxalate was sufficient to increase 4T1 cell adhesion in vitro. However, this effect was significantly alleviated by the addition of DNAse I to scavenge NETs. It has been reported that NET-DNA acts as a chemotactic factor to attract disseminating cancer cells[18]. Our results showed that NETs derived from oxalate-treated neutrophils recruited more 4T1 cells, while digesting NET DNA with DNAse I attenuated this effect (Figure 4G). Subsequently, we investigated the role of NETs in oxalate-induced lung PMN formation. DNAse I was injected intravenously into mice that inhaled oxalate to degrade NETs. Two hours later, 4T1 cells were injected into the mice via the tail vein and lung metastases were detected. Obviously, administration of DNAse I abolished the prometastatic effect of oxalate (Figure 4H). Taken together, these data demonstrated that HAO1-induced oxalate accumulation led to NET formation in the lung PMN.

Oxalate accumulation promotes the proliferation of metastatic cancer cells by activating MAPK signaling

A previous study has suggested that oxalate treatment promotes breast cancer growth[6]. We detected the proliferation of 4T1 and MDA-MB-231 cells under treatment with different doses of oxalate in vitro. The results of the colony formation assay showed that oxalate could stimulate the proliferation of breast cancer cells, especially at a concentration of 20 μM (Figure 5A and B). Metastatic lesions of 4T1 cells were detected in the lungs of mice that inhaled oxalate and showed enhanced proliferation (shown using Ki-67) (Figure 5C). However, CCPST administration dampened the proliferation of metastatic lesions in the lung of 4T1-bearing mice (Figure 5D). These results suggested that exposure of breast cancer cells to oxalate promoted cancer outgrowth. To reveal the potential mechanisms by which oxalate induced breast cancer cell proliferation, we performed RNA-Seq to screen the differentially expressed genes in 4T1 cells treated with oxalate. We identified 959 differentially expressed genes and found that genes upregulated in oxalate-treated 4T1 cells were associated with the MAPK signaling pathway (Figure 5E). Western blot analysis confirmed that the phosphorylation levels of p38 were up-regulated in oxalate-treated 4T1 cells, suggesting that oxalate activated MAPK signaling pathway (Figure 5F). We then isolated mCherry-expressing 4T1 cells from the lungs of 4T1-bearing mice treated with CCPST by FACS. CCPST administration led to MAPK signaling pathway inactivation in pulmonary metastatic 4T1 cells (Figure 5G). Next, SB 203580, an inhibitor of p38 MAPK, was applied to inactivate the MAPK signaling pathway in 4T1 cells. The results of the colony formation assay showed that SB 203580 treatments markedly suppressed the promotion of 4T1 cell proliferation induced by oxalate (Figure 5H). These results

indicated that oxalate accumulation promoted the proliferation of metastatic cancer cells by activating the MAPK signaling pathway.

Primary cancer induces HAO1 expression in alveolar epithelial cells by activating TLR3-IRF3 signaling

Finally, we explored the mechanism by which primary cancer induces HAO1 expression in alveolar epithelial cells. Primary tumors can induce PMN formation at foreign sites by releasing exosomes, which are defined as lipid-bilayer vesicles containing protein, RNA, and DNA[1, 26]. To examine whether exosomes were involved in tumor-induced HAO1 expression, we derived exosomes from 67NR and 4T1 cells for further study (Supplementary figure 6A and B). Apparently, exosomes from 4T1 cells, but not those from 67NR, led to increased HAO1 expression in alveolar epithelial cells (Figure 6A). Moreover, we also observed elevalted HAO1 expression in alveolar epithelial cells transfected with RNA isolated from 4T1-derived exosomes (Figure 6B). A previous study has shown that activation of TLR3 in alveolar epithelial cells is critical for initiating neutrophil recruitment and lung metastatic niche formation by sensing tumor exosomal double-stranded RNA (dsRNA) [21]. We asked whether TLR3 was involved in the regulation of HAO1 expression in alveolar epithelial cells. We treated alveolar epithelial cells with poly (I:C), an agonist of TLR3. Western blot and qPCR analysis showed that the expression of HAO1 in alveolar epithelial cells was significantly increased by poly(I:C) treatment (Figure 6C, supplementary figure 6C). Congruently, inhalation of poly(I:C) in mice resulted in a significant upregulation of HAO1 in lung (Figure 6D, supplementary figure 6D). Moreover, poly(I:C) incubation promoted oxalate production in alveolar epithelial cells, while CCPST treatment reversed this effect (Figure 6E). Then, alveolar epithelial cells were incubated with 4T1-derived exosomes in vitro and CU CPT 4a (inhibitor of TLR3) was applied to block TLR3. The results showed that pharmacological inhibition of TLR3 abolished 4T1-derived exosome-induced HAO1 expression and oxalate production in alveolar epithelial cells (Figure 6F and G).

To investigate the mechanism through which TLR3 modulates HAO1 expression, we analyzed transcription factors located within a 2-kb region directly upstream of the transcription start site of HAO1 using the TFtarget database. In the promoter of HAO1, several binding motifs were found for IRF3, the major transcription factor activated by TLR3 (Figure 6H). A luciferase reporter assay showed that over-expression of IRF3 led to elevated luciferase activity of the HAO1 promoter in alveolar epithelial cells (Figure 6I). In addition, over-expression of IRF3 in alveolar epithelial cells markedly increased the expression of HAO1 (Figure 6J, supplementary figure 6E). These results verified that IRF3 increased the promoter activity of HAO1. We then knocked down IRF3 expression in alveolar epithelial cells treated with poly(I:C) or incubated with 4T1-derived exosomes. Western blot analysis suggested that IRF3 knockdown hampered HAO1 expression induced by poly(I:C) or 4T1-derived exosomes (Figure 6K, supplementary figure 6F). Moreover, IRF3 knockdown resulted in a dramatic reduction of oxalate in alveolar epithelial cells treated with poly(I:C) or incubated with 4T1-derived exosomes (Figure 6L, supplementary figure 6G). These findings illustrated that TLR3-IRF3 signaling was necessary for HAO1 expression and oxalate production in alveolar epithelial cells induced by metastatic breast cancer cells.

Discussion

Cancer-induced metabolic reprogramming has been shown to be involved in PMN-promoted cancer metastasis[1, 2, 27]. Reprogramming of glucose metabolism in recipient PMN cells promotes the development of metastasis[2]. However, the impact of the enriched metabolic components in pre-metastatic niches on tumor metastasis have been insufficiently explored. In this study, the capacity of HAO1-induced oxalate metabolism to promote the formation of lung PMNs was demonstrated for the first time.

Oxalate is a potentially toxic dicarboxylic acid that is not further metabolized by mammals[3]. Oxalate has been shown to be a tumor promoting factor in breast cancer[6], but its role in cancer progression has not been reported. HAO1 is the key enzyme in the pathway of oxalate production and has the ability to oxidize glycolate to glyoxylate and glyoxylate to oxalate[7, 8, 10]. Suppression of HAO1 has been shown in preclinical models to prevent the formation of calcium oxalate[10, 12, 28]. In this study, we found that metastatic breast cancer selectively elevated HAO1 expression in lung alveolar epithelial cells, which led to oxalate accumulation in the lung PMN. Alveolar epithelial cells not only serve as a biological barrier in the respiratory tract, but also play an essential role in the recognition of injury-associated signals, orchestrating innate immunity in the lung[29]. Oxalate accumulation promoted the release of many proinflammatory and prometastatic factors in lung tissue and ultimately lung metastatic colonization. Then, we evaluated whether inhibition of HAO1 could be used to prevent lung metastasis of cancer. Administration of CCPST, a HAO1 inhibitor, has been previously described as a feasible strategy to reduce oxalate production both in vivo and in vitro[10]. Our data showed that CCPST and AAV6-Hao1 sgRNA suppressed oxalate production in lung PMNs induced by metastatic breast cancer and lung metastasis. These results suggest that HAO1 is an eligible therapeutic target to prevent PMN-promoted lung metastasis.

Recent studies have focused on oxalate as an activator of inflammatory pathways[25]. We investigated the effect of HAO1-induced oxalate accumulation on the inflammatory response within lung PMN. We observed the significantly greatest aggregation of neutrophils in lung of mice that inhaied oxalate. The recruitment of neutrophils is considered an essential event in cancer-induced PMN formation[30]. A previous study has revealed that oxalate induces oxidative stress by the production of ROS via NADPH oxidase[4]. In neutrophils, NET formation depends on the generation of ROS by NADPH oxidase[13], which promotes cancer metastasis by trapping disseminating tumor cells and activating the CCDC25-ILK-β-parvin-RAC1-CDC42 cascade in cancer[16, 18]. Hence, we assumed that oxalate accumulation within the lung PMN might contribute to metastasis by inducing NET formation. As expected, our results showed that HAO1-induced oxalate accumulation promoted NET formation in the lung PMN and attracted disseminating cancer cells. However, degradation of NETs by DNAse I hampered the pro-metastatic effect of oxalate and inhibited lung metastatic colonization in mice.

It has been reported that chronic exposure of breast epithelial cells to oxalate promotes the transformation of breast cells from normal to tumor cells, inducing the expression of proto-oncogenes such as c-fos and proliferation in breast cancer cells[6]. We also confirmed that oxalate accumulation

promoted the growth of breast cancer in vitro and in vivo. RNA-Seq analyses showed that HAO1-induced oxalate accumulation enhanced the proliferation of breast cancer cells mainly by activating MAPK signaling. MAPK regulates the expression of genes involved in many processes that play a key role in the development and progression of cancer, such as proliferation, migration and apoptosis[31]. We found that inhibition of the MAPK signaling pathway markedly suppressed the proliferation of cancer cells induced by oxalate.

Exosomes derived from primary tumors are critical for PMN formation in distant organs[1, 26]. We found that stimulation of 4T1-derived exosomes or transfection of exosomal RNA from 4T1 cells was sufficient to induce HAO1 expression in alveolar epithelial cells. A recent study has shown that tumor exosomal RNAs promote lung PMN formation by activating TLR3, which is predominantly expressed by alveolar epithelial cells in pre-metastatic lungs[21]. TLRs can recognize exogenous and endogenous stimulators to prime immune responses[32]. As sensors for dsRNA, tumor TLR3 promotes tumor cell survival, proliferation and chemotherapy resistance[33], or improves sensitivity to poly(I:C)-mediated cancer therapy[34]. We investigated the role of TLR3 signaling in the up-regulation of HAO1 in alveolar epithelial cells and found that TLR3 signaling was required for HAO1 expression in alveolar epithelial cells induced by primary breast cancer. High expression of lung epithelial TLR3 is related to smoke-induced chronic inflammation[35]. We also found that phamacological inhibition of TLR3 abolished breast cancer-induced HAO1 expression and oxalate production. Moreover, our results verified that IRF3, the major transcription factor activated by TLR3, increased promoter activity of HAO1. Knockdown of IRF3 dampened HAO1 expression and oxalate production induced by poly(I:C) or 4T1-derived exosomes. Thus, activation of TLR3-IRF3 signaling promotes HAO1-induced oxalate accumulation in alveolar epithelial cells.

Conclusion

We unveiled an oxalate metabolism-dependent mechanism for lung PMN formation and metastasis (Fig. 6K). Targeting HAO1-mediated oxalate metabolism is a feasible approach to prevent and treat cancer metastasis to the lung.

Abbreviations

HAO1 Hydroxyacid Oxidase 1

NADPH Nicotinamide adenine dinucleotide phosphate

PMN Pre-metastatic niche

NET Neutrophil extracellular trap

DsRNA Double-stranded RNA

TLR3 Toll Like Receptor 3

IRF3 Interferon Regulatory Factor 3

AAV Adeno-associated virus

CCPST 4-carboxy-5-[(4-chlorophenyl)sulfanyl]-1,2,3-thiadiazole

Declarations

Ethics approval and consent to participate

Prior approval was obtained from the Southern Medical University Institutional Board (Guangzhou, China). Informed consent was obtained from each patient. All protocols for animal studies were reviewed and approved by the Institutional Animal Care and Use Committee of Southern Medical University.

Consent for publication

Not applicable.

References

1. Liu, Y. & Cao, X. Characteristics and Significance of the Pre-metastatic Niche. Cancer cell 30, 668-681 (2016).
2. Fong, M. et al. Breast-cancer-secreted miR-122 reprograms glucose metabolism in premetastatic niche to promote metastasis. Nature cell biology 17, 183-194 (2015).

3. Robertson, D.S. The function of oxalic acid in the human metabolism. Clinical chemistry and laboratory medicine 49, 1405-1412 (2011).

4. Joshi, S., Peck, A. & Khan, S. NADPH oxidase as a therapeutic target for oxalate induced injury in kidneys. Oxidative medicine and cellular longevity 2013, 462361 (2013).

5. H, T. et al. Involvement of renin-angiotensin-aldosterone system in calcium oxalate crystal induced activation of NADPH oxidase and renal cell injury. World journal of urology 34, 89-95 (2016).

6. AM, C. et al. Oxalate induces breast cancer. BMC cancer 15, 761 (2015).

7. Schnedler, N., Burckhardt, G. & Burckhardt, B. Glyoxylate is a substrate of the sulfate-oxalate exchanger, sat-1, and increases its expression in HepG2 cells. Journal of hepatology 54, 513-520 (2011).

8. Baker, P., Cramer, S., Kennedy, M., Assimos, D. & Holmes, R. Glycolate and glyoxylate metabolism in HepG2 cells. American journal of physiology. Cell physiology 287, C1359-1365 (2004).

9. N, Z. et al. CRISPR/Cas9-mediated glycolate oxidase disruption is an efficacious and safe treatment for primary hyperoxaluria type I. Nature communications 9, 5454 (2018).

10. Martin-Higueras, C., Luis-Lima, S. & Salido, E. Glycolate Oxidase Is a Safe and Efficient Target for Substrate Reduction Therapy in a Mouse Model of Primary Hyperoxaluria Type I. Molecular therapy : the journal of the American Society of Gene Therapy 24, 719-725 (2016).

11. JM, B. et al. Structure of human glycolate oxidase in complex with the inhibitor 4-carboxy-5-[(4-chlorophenyl)sulfanyl]-1,2,3-thiadiazole. Acta crystallographica. Section F, Structural biology and crystallization communications 65, 1246-1253 (2009).

12. A, L. et al. An Investigational RNAi Therapeutic Targeting Glycolate Oxidase Reduces Oxalate Production in Models of Primary Hyperoxaluria. Journal of the American Society of Nephrology : JASN 28, 494-503 (2017).

13. Fuchs, T. et al. Novel cell death program leads to neutrophil extracellular traps. The Journal of cell biology 176, 231-241 (2007).

14. Jorch, S. & Kubes, P. An emerging role for neutrophil extracellular traps in noninfectious disease. Nature medicine 23, 279-287 (2017).

15. Lee, W. & Naora, H. Neutrophils fertilize the pre-metastatic niche. Aging 11, 6624-6625 (2019).

16. Cools-Lartigue, J. et al. Neutrophil extracellular traps sequester circulating tumor cells and promote metastasis. The Journal of clinical investigation (2013).

17. Teijeira, Á. et al. CXCR1 and CXCR2 Chemokine Receptor Agonists Produced by Tumors Induce Neutrophil Extracellular Traps that Interfere with Immune Cytotoxicity. Immunity 52, 856-871.e858 (2020).

18. Yang, L. et al. DNA of neutrophil extracellular traps promotes cancer metastasis via CCDC25. Nature 583, 133-138 (2020).

19. Alexopoulou, L., Holt, A., Medzhitov, R. & Flavell, R. Recognition of double-stranded RNA and activation of NF-kappaB by Toll-like receptor 3. Nature 413, 732-738 (2001).

20. Valadi, H. et al. Exosome-mediated transfer of mRNAs and microRNAs is a novel mechanism of genetic exchange between cells. Nature cell biology 9, 654-659 (2007).

21. Y, L. et al. Tumor Exosomal RNAs Promote Lung Pre-metastatic Niche Formation by Activating Alveolar Epithelial TLR3 to Recruit Neutrophils. Cancer cell 30, 243-256 (2016).

22. Tavora, B. et al. Tumoural activation of TLR3-SLIT2 axis in endothelium drives metastasis. Nature 586, 299-304 (2020).

23. Zeng, Z. et al. Cancer-derived exosomal miR-25-3p promotes pre-metastatic niche formation by inducing vascular permeability and angiogenesis. Nature communications 9, 5395 (2018).

24. Kowanetz, M. et al. Granulocyte-colony stimulating factor promotes lung metastasis through mobilization of Ly6G+Ly6C+ granulocytes. Proceedings of the National Academy of Sciences of the United States of America 107, 21248-21255 (2010).

25. J, Z. et al. Inhibiting inflammation and modulating oxidative stress in oxalate-induced nephrolithiasis with the Nrf2 activator dimethyl fumarate. Free radical biology & medicine 134, 9-22 (2019).

26. Peinado, H. et al. Pre-metastatic niches: organ-specific homes for metastases. Nature reviews. Cancer 17, 302-317 (2017).

27. Wu, Z. et al. TPO-Induced Metabolic Reprogramming Drives Liver Metastasis of Colorectal Cancer CD110+ Tumor-Initiating Cells. Cell stem cell 17, 47-59 (2015).

28. Dutta, C. et al. Inhibition of Glycolate Oxidase With Dicer-substrate siRNA Reduces Calcium Oxalate Deposition in a Mouse Model of Primary Hyperoxaluria Type 1. Molecular therapy : the journal of the American Society of Gene Therapy 24, 770-778 (2016).

29. Whitsett, J. & Alenghat, T. Respiratory epithelial cells orchestrate pulmonary innate immunity. Nature immunology 16, 27-35 (2015).

30. Jablonska, J., Lang, S., Sionov, R. & Granot, Z. The regulation of pre-metastatic niche formation by neutrophils. Oncotarget 8, 112132-112144 (2017).

31. Yuan, J., Dong, X., Yap, J. & Hu, J. The MAPK and AMPK signalings: interplay and implication in targeted cancer therapy. Journal of hematology & oncology 13, 113 (2020).

32. Kawai, T. & Akira, S. The role of pattern-recognition receptors in innate immunity: update on Toll-like receptors. Nature immunology 11, 373-384 (2010).

33. Sistigu, A. et al. Cancer cell-autonomous contribution of type I interferon signaling to the efficacy of chemotherapy. Nature medicine 20, 1301-1309 (2014).

34. Forte, G. et al. Polyinosinic-polycytidylic acid limits tumor outgrowth in a mouse model of metastatic lung cancer. Journal of immunology (Baltimore, Md. : 1950) 188, 5357-5364 (2012).

35. Milara, J. et al. Roflumilast improves corticosteroid resistance COPD bronchial epithelial cells stimulated with toll like receptor 3 agonist. Respiratory research 16, 12 (2015).
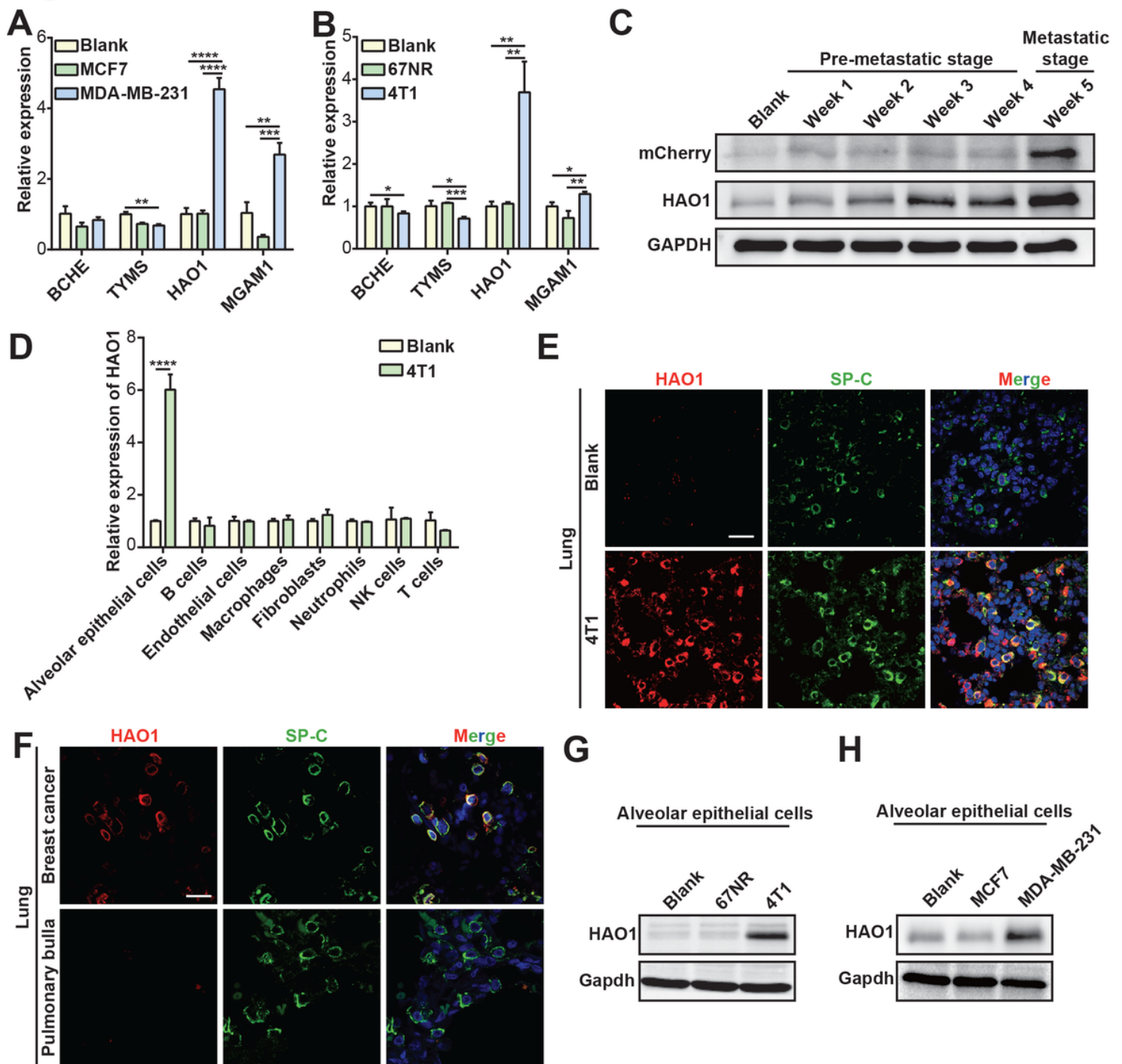
Figures

Figure 1

Figure 1

Primary cancer induces pulmonary HAO1 expression. (A and B) QPCR analysis of HAO1、MGAM、BCHE and TYMS expression in lungs from mice without tumor (blank) and mice bearing MCF7, MDA-MB-231 (A), 67NR, 4T1 cells (B) for 2 weeks. Means ± s.e.m are provided (n=3). (C) Western blot analysis of mCherry and HAO1 expression in lungs from mice without tumor and mice bearing mCherry-expressing 4T1 cells for 1 to 5 weeks. (D) QPCR analysis of HAO1 expression in alveolar epithelial cells, B cells, endothelial cells, macrophages, fibroblast, neutrophils, NK cells and T cells of lung from control mice and

mice bearing 4T1 cells for 2 weeks. Means ± s.e.m are provided (n=3). (E) Immunofluorescence staining of HAO1 (red) and SP-C (green) in lungs from mice bearing 4T1 cells for 2 weeks. Scale bars, 20 μm. (F) Immunofluorescence staining of HAO1 (red) and SP-C (green) in lung tissue derived from breast cancer patients with lung metastases and patients with pulmonary bulla. Scale bars, 20 μm. (G and H) Western blot analysis of HAO1 expression in alveolar epithelial cells cocultured with 67NR, 4T1 (G), MCF7 and MDA-MB-231 cells(H). *P<0.05, **P<0.01, ***P<0.001, ****P<0.0001 according to the two-tailed Student's t-test.
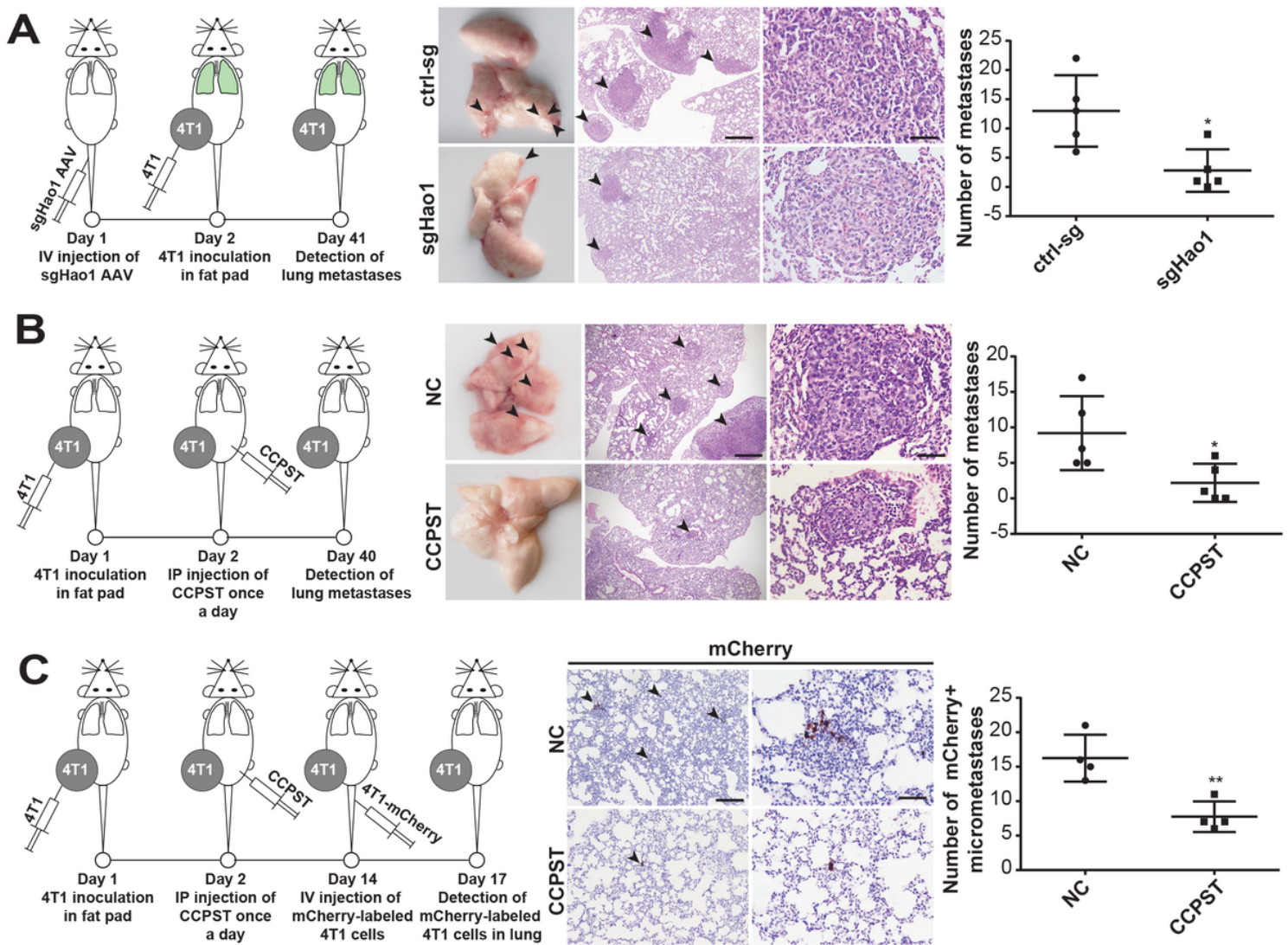
Figure 2

Figure 2

HAO1 induces lung PMN formation. (A) Effect of AAV6-Hao1 sgRNA treatment on lung metastasis in mice bearing 4T1 cells. Means ± s.e.m are provided (n=5). The scale bar in the middle panels represents 200 μm. The scale bar in right panels represents 20 μm. (B) Effect of CCPST treatment on lung metastasis in mice bearing 4T1. Means ± s.e.m are provided (n=5). The scale bar in the middle panels represents 200 μm. Scale bar in the right panels represents 20 μm. (C) MCherry-labeled 4T1 cells were injected into tail vein of mice 2 weeks after inoculation of unlabeled 4T1 cells into fat pad and once daily

administration of CCPST. Quantitation of the number of tumor foci identified by mCherry staining of lung histologic sections. Mean ± s.e.m are provided (n=4). The scale bar in the left panels represents 200 μm. The scale bar in the right panels represents 20 μm. *P<0.05, **P<0.01 according to two-tailed Student's t-test.
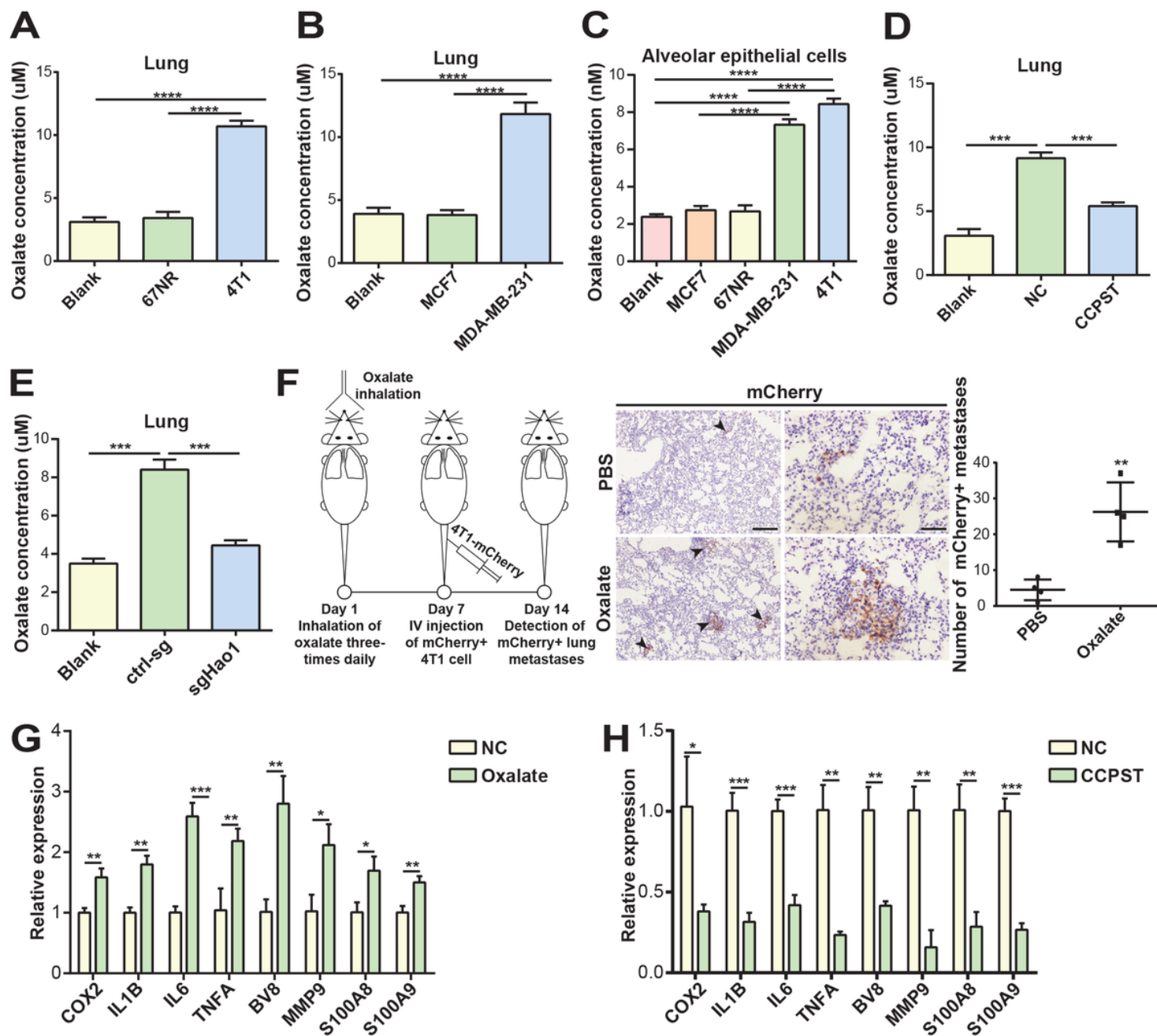
Figure 3

Figure 3

HAO1 promotes oxalate production in the lung PMN. (A and B) Detection of oxalate concentration in lungs from mice without tumor (blank) and mice bearing 67NR, 4T1 (A), MCF7 and MDA-MB-231 cells (B) for 2 weeks. Means ± s.e.m are provided (n=3). (C) Detection of the oxalate concentration in alveolar epithelial cells cocultured with 67NR, 4T1, MCF7 and MDA-MB-231 cells. Means ± s.e.m are provided

(n=3). (D) Effect of CCPST treatment on pulmonary oxalate production in mice bearing 4T1 cells. Mean ± s.e.m are provided (n=4). (E) Effect of AAV6-Hao1 sgRNA treatment on pulmonary oxalate production in mice bearing 4T1 cells. Means ± s.e.m are provided (n=3). (F) MCherry-labeled 4T1 cells were injected into the tail vein of mice that had inhaled PBS or oxalate. The number of tumor foci was determined by mCherry staining of lung tissue sections. Means ± s.e.m are provided (n=4). Scale bar in left panels represents 200 μm. The scale bar in right panels represents 20 μm. (G) QPCR analysis of COX2, IL1B, IL6, TNFa, Bv8, MMP9, S100a8 and S100a9 expression in lungs from control mice and mice receiving oxalate inhalation three-times daily for one week. Means ± s.e.m are provided (n=3). (H) QPCR analysis of COX2, IL1B, IL6, TNFa, Bv8, MMP9, S100a8 and S100a9 expression in lungs from 4T1-bearing mice receiving once daily administration of CCPST. Means ± s.e.m are provided (n=3). *P<0.05, **P<0.01, ***P<0.001, ****P<0.0001 according to the two-tailed Student's t-test.
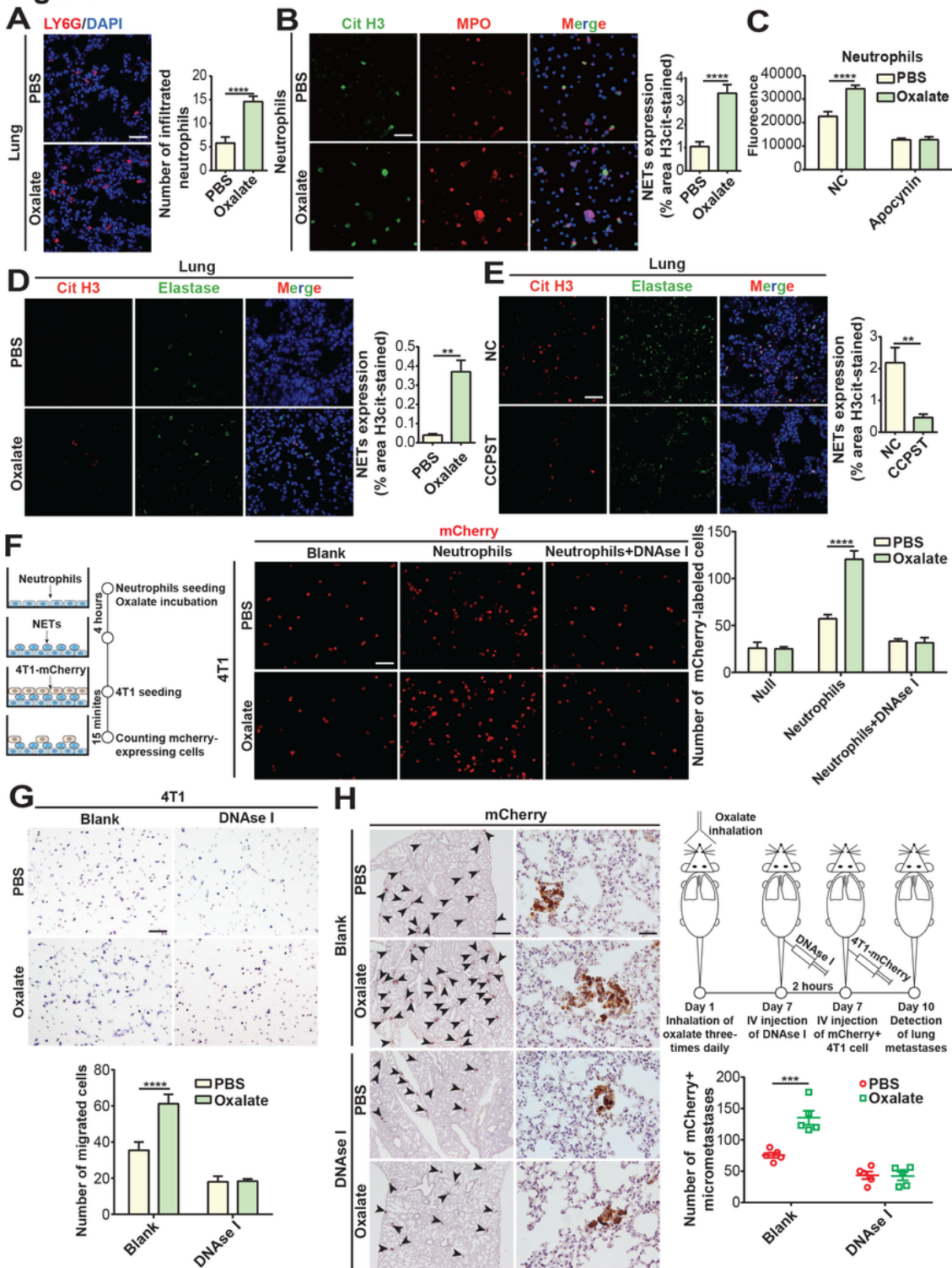
Figure 4

Figure 4

Oxalate accumulation induces NET formation. (A) Images and quantification of neutrophils (labeled by LY6G, red) in the lungs from control mice and mice that received oxalate inhalation three times daily for one week. Scale bars, 20 μm. Means ± s.e.m are provided (n = 5). (B) Detection of NETs by immunofluorescence in neutrophils incubated with PBS or oxalate. NETs were defined as colocalized MPO (red), citrullinated histone H3 (green), and DNA (blue). Scale bars, 20 μm. Means ± s.e.m are

provided (n = 5). (C) Detection of ROS production in neutrophils incubated with PBS or oxalate. Mean ± s.e.m are provided (n = 3). (D) Effect of oxalate inhalation on NET formation in mice lungs. NETs were defined as colocalized citrullinated histone H3 (red), elastase (green), and DNA (blue). Scale bars, 20 µm. Means ± s.e.m are provided (n = 5). (E) Effect of CCPST treatment on NET formation in lungs from mice bearing 4T1 cells. Scale bars, 20 µm. Means ± s.e.m are provided (n = 5). (F) Images and quantification of 4T1 cells (labeled by mCherry, red) adhering to neutrophils incubated with PBS or oxalate for 4 h. Scale bars, 20 µm. Means ± s.e.m are provided (n = 5). (G) Images and quantification of 4T1 cells that migrated to NETs derived from neutrophils incubated with PBS or oxalate for 4 h. Scale bars, 20 µm. Mean ± s.e.m are provided (n = 5). (H) MCherry-labeled 4T1 cells were injected into the tail vein of mice receiving PBS inhalation, oxalate inhalation, PBS inhalation + DNAse I injection or oxalate inhalation + DNAse I injection. The number of tumor foci was determined by mCherry staining of lung tissue sections. Means ± s.e.m are provided (n=5). The scale bar in left panels represents 200 µm. Scale bar in right panels represents 20 µm. **P<0.01, ***P<0.001, ****P<0.0001 according to the two-tailed Student's t-test.
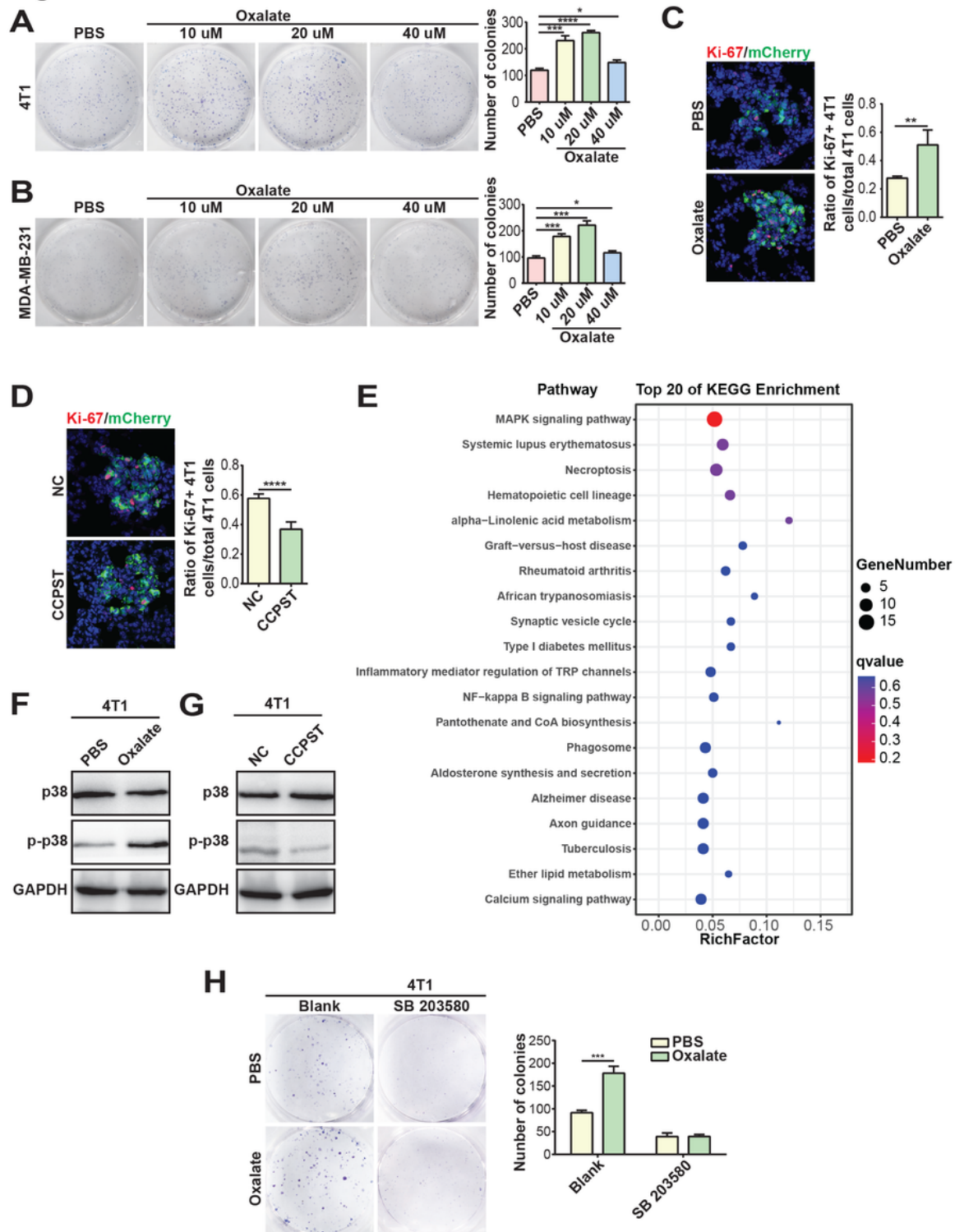
Figure 5

Figure 5

Oxalate accumulation promotes the proliferation of metastatic cancer cells. (A and B) Effect of oxalate treatment on the proliferation of 4T1 (A) and MDA-MB-231 cells (B). Means ± s.e.m are provided (n = 3). (C) Ratio of Ki-67+ 4T1 cells (red)/total 4T1 cells (labeled by mCherry, green) in lungs from mice inhaled PBS or oxalate. Means ± s.e.m are provided (n=5). Scale bar, 20 μm. (D) Ratio of Ki-67+ 4T1 cells (red)/total 4T1 cells (labeled by mCherry, green) in lungs from mice receiving a once daily administration

of CCPST. Means ± s.e.m are provided (n=5). Scale bar, 20 μm. (E) KEGG pathway enrichment analysis of differentially expressed genes between 4T1 cells incubated with PBS or oxalate. (F) Effect of oxalate treatment on total p38 expression and p38 phosphorylation in 4T1 cells. (G) Effect of CCPST treatment on total p38 expression and p38 phosphorylation in metastatic 4T1 cells from lungs of tumor-bearing mice. (H) Changes in the growth rate in 4T1 treated with PBS, oxalate, SB 203580 + PBS or SB 203580 + oxalate. Means ± s.e.m are provided (n = 3). *P<0.05, **P<0.01, ***P<0.001, ****P<0.0001 according to the two-tailed Student's t-test.
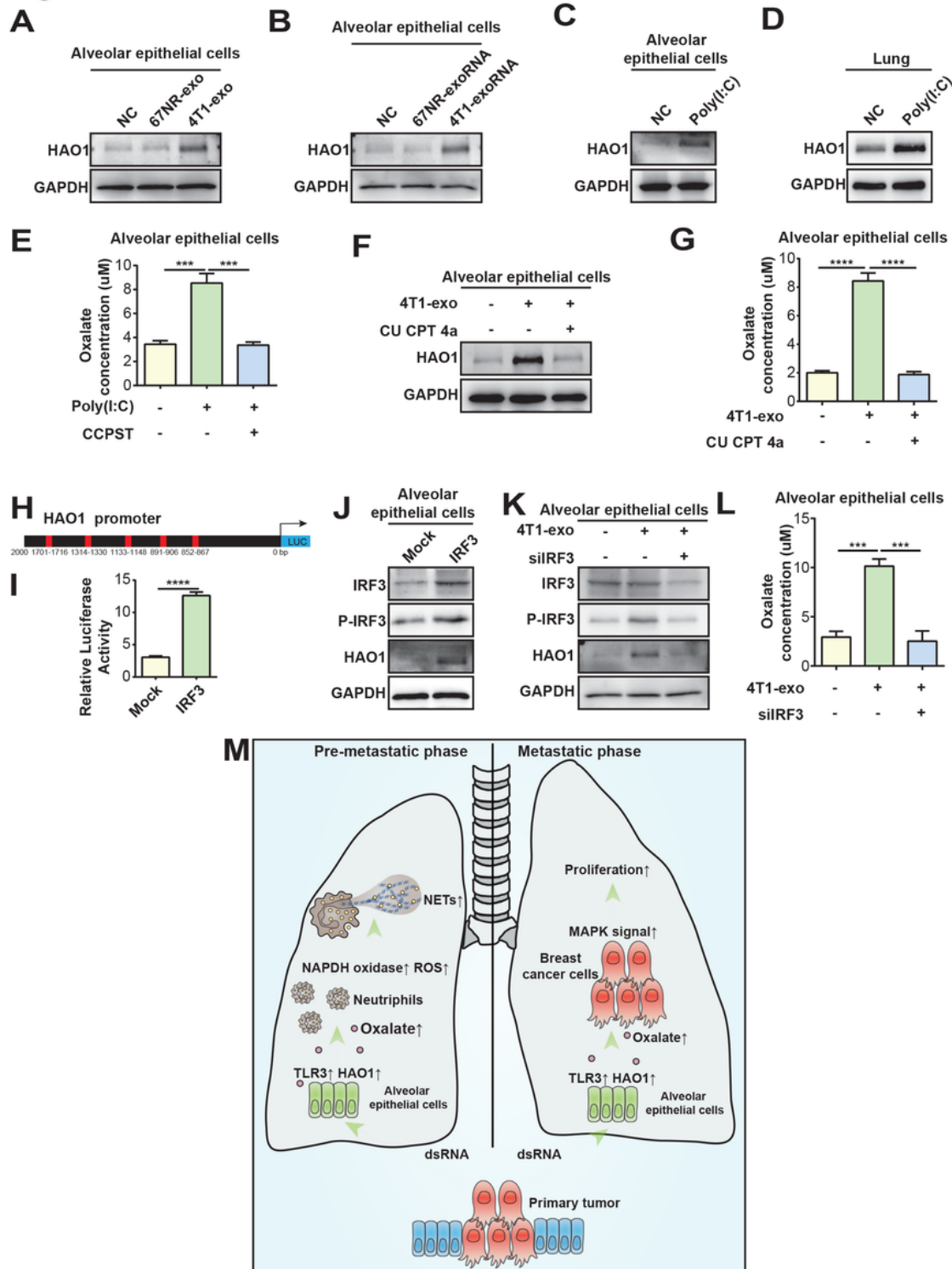
Figure 6

Figure 6

TLR3 signal activation induces HAO1 expression in alveolar epithelial cells. (A) Effect of 67NR and 4T1 exosomes treatment on HAO1 expression in alveolar epithelial cells by Western blot analysis. (B) Effect of transfection of RNA isolated from 67NR and 4T1 exosomes on HAO1 expression in alveolar epithelial cells by Western blot analysis. (C) Effect of poly (I:C) treatment on HAO1 expression in alveolar epithelial cells by Western blot analysis. (D) Effect of poly (I:C) inhalation on HAO1 expression in mice lung by Western blot analysis. (E) Detection of oxalate production in alveolar epithelial cells treated with poly(I:C) or poly(I:C) + CCPST. Means ± s.e.m are provided (n = 3). (F) Detection of HAO1 expression in alveolar epithelial cells treated with 4T1 exosomes or 4T1 exosomes + CU CPT 4a by Western blot analysis. (G) Detection of oxalate production in alveolar epithelial cells treated with 4T1 exosomes or 4T1 exosomes + CU CPT 4a. (H) Diagram of the HAO1 promoter showing the location of IRF3 binding sites. (I) Luciferase activity of HAO1-promoter construct after transfection of IRF3 plasmid in alveolar epithelial cells. (J) Effect of IRF3 over-expressiom on IRF3, P-IRF3 and HAO1 expression in alveolar epithelial cells by Western blot analysis. (K) Detection of IRF3, P-IRF3 and HAO1 expression in alveolar epithelial cells treated with 4T1 exosomes or 4T1 exosomes + siIRF3 by Western blot analysis. (L) Detection of oxalate production in alveolar epithelial cells treated with 4T1 exosomes or 4T1 exosomes + siIRF3. Means ± s.e.m are provided (n = 3). (M) Schematic diagram of the role of HAO1-mediated oxalate metabolism at pre-metastatic stage and metastatic stage. ***$P<0.001$, ****$P<0.0001$ according to two-tailed Student's t-test.

Supplementary Files

This is a list of supplementary files associated with this preprint. Click to download.

- SupplementaryInformation.pdf